Bioorganic & Medicinal Chemistry Letters 24 (2014) 1511–1518

Contents lists available at ScienceDirect

Bioorganic & Medicinal Chemistry Letters

journal homepage: www.elsevier.com/locate/bmcl

Synthesis and antitumor activities of novel dipeptide derivatives derived from dehydroabietic acid

Xiao-Chao Huang [a,†], Meng Wang [a,†], Heng-Shan Wang [a], Zhen-Feng Chen [a], Ye Zhang [a,b,*], Ying-Ming Pan [a,*]

[a] State Key Laboratory Cultivation Base for the Chemistry and Molecular Engineering of Medicinal Resources, School of Chemistry & Pharmaceutical Science of Guangxi Normal University, Yucai Road 15, Guilin 541004, Guangxi, PR China
[b] Department of Chemistry & Pharmaceutical Science, Guilin Normal College, Xinyi Road 15, Guangxi 541001, PR China

ARTICLE INFO

Article history:
Received 31 October 2013
Revised 20 January 2014
Accepted 1 February 2014
Available online 10 February 2014

Keywords:
Dehydroabietic acid
Dipeptide
Cytotoxicity
Apoptosis

ABSTRACT

A series of dipeptide derivatives from dehydroabietic acid were designed and synthesized as novel antitumor agents. The antitumor activities screening indicated that many compounds showed moderate to high levels of inhibition activities against NCI-H460, HepG2, SK-OV-3, BEL-7404, HeLa and HCT-116 cancer cell lines and that some displayed more potent inhibitory activities than commercial anticancer drug 5-fluorouracil. The mechanism of representative compound **7b** was studied by AO/EB staining, Hoechst 33258 staining, JC-1 mitochondrial membrane potential staining, TUNEL assay, DNA ladder assay and flow cytometry, which exhibited that the compound could induce apoptosis in HeLa cells. Further investigation showed that compound **7b** induced apoptosis of HeLa cells through a mitochondrial pathway.

Cancer is one of the primary causes of death globally, so searching and developing effective anticancer drugs have greatly attracted bioorganic chemists' interest. After the success of vinblastine, taxol and their related derivatives as antitumor drugs, natural products have been seriously considered as a good traditional source of new antitumor drugs.[1–6]

As a natural occurring diterpenic resin acid, dehydroabietic acid (DHA) and its derivatives has been found to have properties of enhancing the inhibition activity of anticancer drug in various cells, such as hepatocellular carcinoma cells, cervical carcinoma cells, and breast cancer cells.[7] Our previous study has also demonstrated that DHA could be a useful tool in the synthesis of drugs active against some tumour cells.[8] Continuing our research program on the synthesis of antitumor drugs effective, DHA skeleton is chosen in the present work as active structural core and some structural modifications are carried out to explore their antitumor activities. Dipeptide, an important versatile bioactive moiety,[9] is able to improve the antitumor activity by constructing on a pharmacy core.[10–13] Many dipeptide derivatives have exhibited potent inhibition activities against human tumors cells.[9a,10–12] It is thus to expect that introducing of dipeptide group on DHA skeleton may contribute to potential antitumor activity. However, the study on the synthesis, antitumor activities and apoptosis-inducing effects of dipeptide derivatives derived from DHA has not been described. Our present work in this paper is to design and synthesize a series of DHA-dipeptide derivatives, and to evaluate their in vitro antitumor activities. Furthermore, the mechanism of apoptotic effects induced by the representative compound **7b** is also investigated.

DHA-dipeptide derivatives were synthesized as outlined in Scheme 1. Compound **2** was synthesized by the treatment of phenylalanine **1** with phthalic anhydride in the presence of acetic acid according to the literature.[13] Compound **3** was then obtained by the condensation of compound **2** and oxalyl chloride, and it was then treated with series of aromatic primary amines to offer compounds **4**. Compounds **5** were synthesized by the treatment of compounds **4** with hydrazine hydrate in the presence of ethanol at room temperature. DHA was treated with oxalyl chloride to offer compound **6**. Finally, compounds **7** were acquired by the condensation of compound **6** and compounds **5** in the presence of triethylamine at room temperature. The structures of DHA-dipeptide derivatives **7** were confirmed by ^{1}H NMR, ^{13}C NMR and high resolution mass spectrum (HRMS).[14]

The in vitro antitumor activities of DHA-dipeptide derivatives **7a**–**7s** were evaluated by 3-(4,5-dimethylthiazol-2-yl)-2,5-diphenyltetrazolium bromide (MTT)[9,15] assay against NCI-H460, HepG2, SK-OV-3, BEL-7404, HeLa and HCT-116 tumor cell lines, with 5-fluorouracil (5-FU) as the positive control. The tested results were shown in Table 1.

* Corresponding authors. Tel./fax: +86 0773 2120958.
E-mail addresses: zhangye81@126.com (Y. Zhang), panym2005@sina.com (Y.-M. Pan).
† Co-first author: These authors contributed equally to this work.

http://dx.doi.org/10.1016/j.bmcl.2014.02.001
0960-894X/

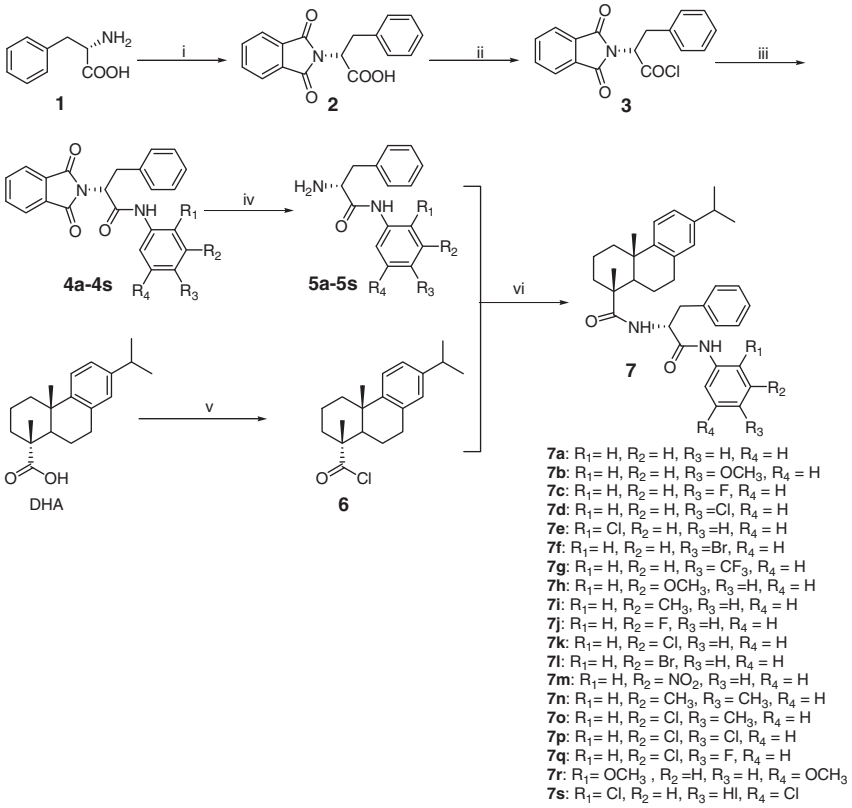

Scheme 1. Synthetic route to target compounds **7a**–**7s**. Reagents and conditions: (i) phthalic anhydride, CH_3COOH, 50 °C; (ii) $(COCl)_2$, CH_2Cl_2, rt; (iii) aromatic primary amines, Et_3N, CH_2Cl_2, rt; (iv) $NH_2NH_2{\cdot}H_2O$, CH_3CH_2OH; (v) $(COCl)_2$, CH_2Cl_2, rt; (vi) Et_3N, CH_2Cl_2, rt.

As shown in Table 1, most of DHA-dipeptide derivatives **7a**–**7s** displayed much higher inhibitory activity than DHA against NCI-H460, HepG2, SK-OV-3, BEL-7404, HeLa and HCT-116 cell lines, indicating the introduction of dipeptide group on DHA should markedly improve the antitumor activity. Moreover, the substituent groups at 4-position of phenyl ring (R_4) have important influence on the cytotoxic inhibition and the introduction of electron donor substituents and halogen groups may result in the increase of cytotoxic inhibition, while substituent groups at 3-position of phenyl ring (R_3) may lead to the decrease of cytotoxic inhibition.

Table 1 also revealed that, in NCI-H460 cell line assay, all the compounds exhibited better inhibition than DHA (IC_{50} = 80.53 μM), and most of compounds (such as **7a**–**7g**, **7i**–**7m** and **7o**–**7s**) even displayed preferable cytotoxic activities than the commercial anticancer drug 5-FU (IC_{50} = 36.04 μM), with IC_{50} in the range of 15.21–33.34 μM, indicating good inhibition activities of

Table 1
Effect of compounds **7a**–**7s** against cell viability of different cell lines

Compounds	IC_{50}(μM)					
	NCI-H460	HepG2	SK-OV-3	BEL-7404	HeLa	HCT-116
7a	28.20 ± 1.42	27.71 ± 1.64	27.36 ± 1.57	16.70 ± 0.56	18.89 ± 1.22	30.33 ± 3.26
7b	17.22 ± 1.04	12.40 ± 0.88	23.75 ± 1.76	15.34 ± 0.78	4.94 ± 0.88	15.67 ± 0.76
7c	22.83 ± 2.45	27.10 ± 3.21	20.07 ± 1.22	21.01 ± 1.27	10.84 ± 1.13	27.43 ± 1.39
7d	15.82 ± 1.43	26.30 ± 2.43	26.34 ± 2.34	33.59 ± 2.52	12.22 ± 1.56	37.79 ± 2.78
7e	15.21 ± 1.86	25.26 ± 2.54	13.52 ± 1.33	15.80 ± 2.43	10.29 ± 0.64	25.48 ± 2.65
7f	28.68 ± 1.25	34.64 ± 1.98	28.68 ± 2.46	16.90 ± 2.36	15.20 ± 1.46	35.33 ± 2.31
7g	28.85 ± 2.36	21.61 ± 1.43	36.34 ± 3.54	36.10 ± 2.38	10.47 ± 0.96	27.38 ± 2.56
7h	40.42 ± 3.45	29.50 ± 2.46	30.52 ± 2.13	38.53 ± 3.33	25.79 ± 1.23	35.77 ± 2.45
7i	32.35 ± 2.48	26.90 ± 3.21	29.84 ± 2.12	34.56 ± 3.21	18.19 ± 1.32	32.52 ± 3.21
7j	26.08 ± 3.21	23.86 ± 1.87	33.92 ± 3.14	27.45 ± 2.87	13.91 ± 0.58	34.76 ± 2.12
7k	26.34 ± 2.41	24.65 ± 1.68	30.62 ± 2.76	23.79 ± 2.34	13.06 ± 1.24	45.85 ± 3.15
7l	33.34 ± 3.45	22.89 ± 1.46	38.80 ± 4.21	19.95 ± 2.61	25.13 ± 0.92	44.10 ± 3.65
7m	32.83 ± 2.65	25.26 ± 2.23	20.07 ± 1.23	27.05 ± 2.15	12.82 ± 1.02	27.43 ± 2.31
7n	36.98 ± 3.25	42.78 ± 4.21	51.79 ± 4.56	48.16 ± 3.11	14.34 ± 1.43	32.14 ± 2.41
7o	26.10 ± 2.23	36.90 ± 2.32	37.82 ± 2.31	41.16 ± 3.45	10.11 ± 0.75	32.30 ± 3.42
7p	26.98 ± 2.46	20.42 ± 1.88	33.15 ± 1.27	44.69 ± 2.46	28.79 ± 1.46	40.85 ± 3.67
7q	26.77 ± 2.54	32.91 ± 2.46	30.54 ± 2.85	26.06 ± 2.12	11.12 ± 0.86	39.27 ± 2.55
7r	27.44 ± 2.48	38.07 ± 2.75	53.75 ± 3.51	56.34 ± 3.31	19.26 ± 2.13	36.84 ± 2.56
7s	15.78 ± 1.75	23.43 ± 2.66	21.58 ± 2.18	30.98 ± 2.88	14.94 ± 1.35	24.10 ± 1.29
DHA	80.53 ± 2.11	76.76 ± 3.68	75.00 ± 2.21	34.70 ± 2.23	29.35 ± 2.32	35.24 ± 3.26
5-FU	36.04 ± 2.54	26.98 ± 2.37	24.43 ± 0.41	26.80 ± 2.23	80.48 ± 2.31	24.43 ± 0.40

these compounds on NCI-H460 cell line. The cytotoxic inhibition screening results demonstrated that the introduction of dipeptide moiety on DHA should clearly improve the antitumor activity against NCI-H460 cell line. Among all the compounds, compound **7e** exhibited the best cytotoxicity, with IC_{50} of 15.21 μM.

In HepG2 cell line assay, all compounds displayed better cytotoxicity than DHA (IC_{50} = 76.76 μM), with IC_{50} in the range of 12.40–42.78 μM, indicating that the introduction of dipeptide group on DHA should obviously improve the antitumor activity against HepG2 cell line. Moreover, many compounds (such as **7b**, **7d**, **7e**, **7g**, **7j**–**7m**, **7p** and **7s**) even demonstrated better cytotoxic inhibition than 5-FU, implying favorable inhibition activities of these compounds. Among these compounds, compound **7b** showed the best inhibition, with IC_{50} of 12.40 μM.

In SK-OV-3 cell line assay, all the compounds displayed better cytotoxicity than DHA (IC_{50} = 75.00 μM), with IC_{50} in the range of 13.52–53.75 μM, exhibiting that the introduction of dipeptide fragment on DHA could enhanced the antitumor activity against SK-OV-3 cell line. Moreover, compounds **7b**, **7c**, **7e**, **7m** and **7s** even demonstrated better cytotoxic inhibition than 5-FU. Compound **7e** displayed the best inhibition on SK-OV-3 cell line among all the compounds, with IC_{50} of 13.52 μM.

In BEL-7404 cell line assay, except compounds **7g**, **7h**, **7n**–**7p** and **7r**, other compounds displayed better cytotoxicity than DHA (IC_{50} = 34.70 μM), with IC_{50} in the range of 15.34–34.56 μM, exhibiting that the introduction of dipeptide part on DHA should increase the antitumor activity against BEL-7404 cell line. Moreover, compounds **7a**, **7b**, **7c**, **7e**, **7f**, **7k**, **7l** and **7q** even demonstrated better cytotoxic inhibition than 5-FU, with IC_{50} in the range of 15.34–26.06 μM. Among these compounds, compound **7b** exhibited the best cytotoxic inhibition, with IC_{50} of 15.34 μM.

In HeLa cell line assay, all the compounds displayed better cytotoxicity than DHA (IC_{50} = 29.35 μM), and even preferable than 5-FU, with IC_{50} in the range of 4.94–28.79 μM, exhibiting that the introduction of dipeptide section on DHA should evidently improve the antitumor activity on HeLa cell line. It was important to note that compound **7b** showed the best antitumor activity in this assay, with IC_{50} of 4.94 μM.

In HCT-116 cell line assay, except compounds **7d**, **7f**, **7h**, **7k**, **7l**, **7p**, **7q** and **7r**, other compounds displayed better cytotoxicity than DHA (IC_{50} = 35.24 μM), with IC_{50} in the range of 15.67–34.76 μM, exhibiting that the introduction of dipeptide segment on DHA remarkably improve the antitumor activity against HCT-116 cell line. Moreover, compounds **7b** and **7s** showed better inhibition activity than 5-FU, with IC_{50} of 15.67 and 24.10 μM, respectively.

Apoptosis plays a central role in cancer, since its induction in cancer cells is critical to a successful therapy.[16] It is thus believed that apoptosis assay may provide important information to preliminary investigation of the mode of action. Therefore, in the present study, compound **7b**, which exhibited good cytotoxic inhibition in six cancer cell lines and could be used as a good representative of compounds **7a**–**7s**, was selected and its mechanism of growth inhibition of HeLa cells was evaluated by acridine orange(AO)/ethidium bromide(EB) staining,[17] Hoechst 33258 staining,[18] JC-1 mitochondrial membrane potential staining,[19] TUNEL assay staining[20] and flow cytometry.[21]

AO, which is a vital dye, can stain nuclear DNA across an intact cell membrane, while EB can only stains cells that have lost their membrane integrity. Therefore, after synchronous treating with AO and EB, live cells will be evenly stained as green and early apoptotic cells will be thickly stained as green yellow or show green yellow fragments, while late apoptotic cells will be densely stained as orange or display orange fragments and necrotic cells will be stained as orange. The cytotoxicity of compound **7b** at the concentration of 10 μM against HeLa cells from 12 to 24 h was assayed by AO/EB staining, and HeLa cells not treated with the **7b** were used as control for 24 h. The results were shown in Figure 1. As shown in Figure 1, the HeLa cells treated with **7b** from 12 to 24 h had obviously changed. The nuclei markedly stained as yellow green or orange. The phenomenon was associated with cell apoptosis. Based on the above observation, the cells represented with an apoptotic morphology. These findings indicated that compounds **7b** could induce HeLa cells apoptosis.

Hoechst 33258, which stains the cell nucleus, is a membrane permeable dye with blue fluorescence. Live cells with uniformly light blue nuclei are obviously detected under fluorescence microscope after treatment with Hoechst 33258, whereas apoptotic cells have bright blue nuclei due to karyopyknosis and chromatin condensation. However, the nuclei of dead cells could not be stained. HeLa cells treated with compound **7b** at 10 μM from 12 to 24 h were stained with Hoechst 33258. HeLa cells not treated with the **7b** were used as control at for 24 h. The results were given in Figure 2. As shown in Figure 2, HeLa cells not treated with compound **7b** were normally blue (in the web version). It was worth noting that, for **7b** treatment, the cells displayed strong blue fluorescence and indicated typical apoptotic morphology after 12 and 24 h. The observation revealed that compounds **7b** induced apoptosis against HeLa cell line, consistent with the results for AO/EB double staining.

In order to further investigate the apoptosis-inducing effect of target compound **7b**, mitochondrial membrane potential changes were designed and detected, using the fluorescent probe JC-1. JC-1, which is a lipophilic cationic dye, can easily pass through the plasma membrane into cells and accumulates in actively respiring mitochondria. In the control cells, JC-1 could aggregate in mitochondria and present high red fluorescence. However, in cells undergoing apoptosis, where the mitochondrial potential has collapsed, JC-1 exists in the cytosol as a monomer which emits green fluorescence. HeLa cells treated with compound **7b** at 10 μM from 12 to 24 h were stained with JC-1 and not treated with the compound **7b** were used as control for 24 h. The results were shown in Figure 3. The JC-1 monomer and J-aggregates were excited at 514 and 585 nm, respectively, and light emissions were collected at 515–545 nm (green) and 570–600 nm (red). For fluorescence microscopy, Figure 3 showed that cells not treated with the compound **7b** were normally red (in the web version), while for **7b** treatment, cells showed strong green fluorescence and indicated typical apoptotic morphology after 12 and 24 h. Therefore, it could be concluded that compound **7b** induced apoptosis against HeLa cell line. The results were identical with that of previous experiment of AO/EB double staining and Hoechst 33258 staining.

Terminal-deoxynucleotidyl transferase meditated nick end labeling (TUNEL) is a common method for identifying apoptotic cells in situ by detecting DNA fragmentation. When the genomic DNA is broken, the exposed 3′-OH at the end of deoxynucleotide transfer as the catalytic plus green fluorescent probes fluorescein (FITC) labeled dUTP, which can be detected by fluorescence microscopy or flow cytometry, as indicated by a green color. The results were illustrated in Figure 4. For fluorescence microscopy, Figure 4 revealed that HeLa cells treated with the compound **7b** at different time appeared in green (in the web version), indicating that compound **7b** significantly induced apoptosis against HeLa cell line. The results were consistent well with the previous experiments.

Apoptosis is a fundamental cellular event during development and is critical for the cytotoxicity induced by radiation or drugs characterized by the cleavage of chromatin DNA into inter-nucleosomal fragments. Fragmentation of chromosomal DNA is the biological hallmark of apoptosis[22] and can be detected by gel electrophoresis.[23] The DNA is cleaved to nucleosome-sized fragments of approximately 180–200 base pairs, which results in the formation of a ladder like pattern when the DNA is subjected to

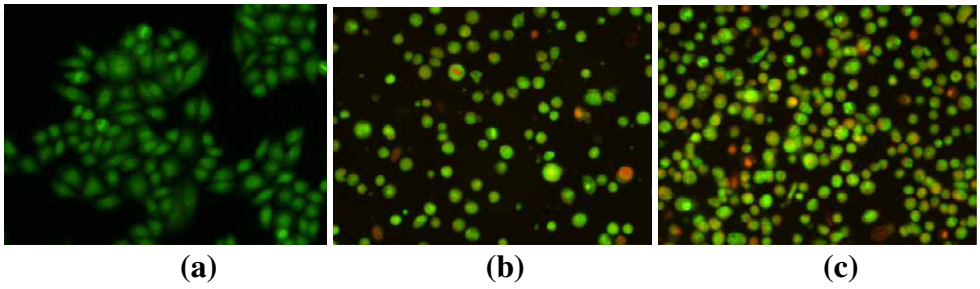

Figure 1. AO/EB staining of compound **7b** in HeLa cells. (a) Not treated with the **7b** was used as control for 24 h and (b, c) treatment with compound **7b** (10 μM) for 12 and 24 h, respectively.

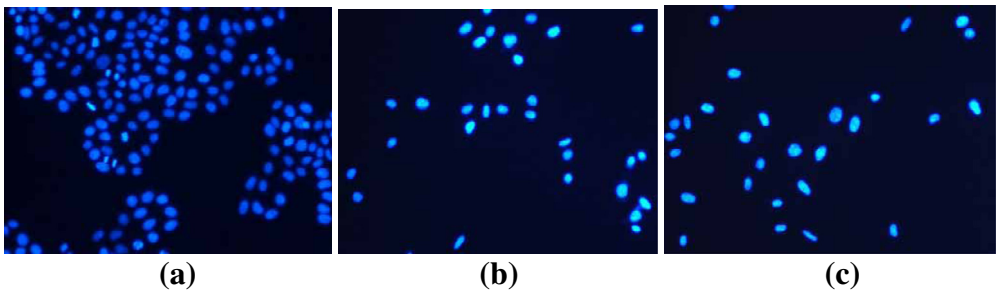

Figure 2. Hoechst 33258 staining of compound **7b** in HeLa cells. (a) Not treated with compound **7b** was used as control for 24 h and (b, c) treatment with compound **7b** (10 μM) for 12 and 24 h, respectively.

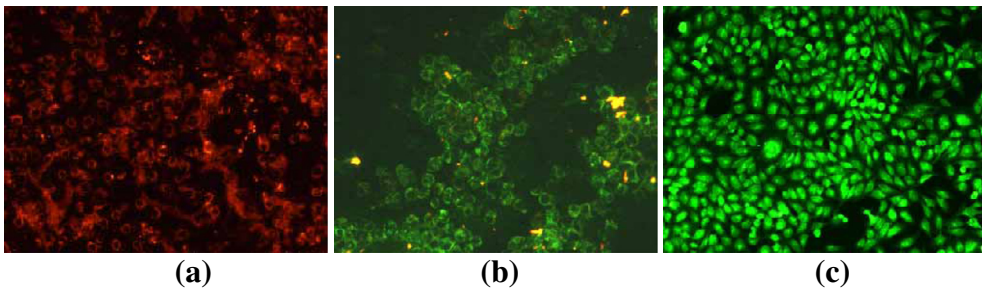

Figure 3. JC-1 mitochondrial membrane potential staining of compound **7b** in HeLa cells. (a) Not treated with the **7b** was used as control for 24 h and (b, c) treatment with compound **7b** (10 μM) for 12 and 24 h, respectively.

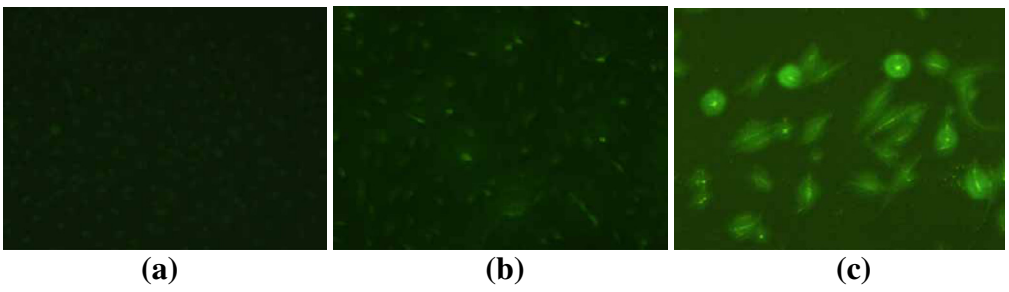

Figure 4. TUNEL assay of compound **7b** in HeLa cells. (a) Not treated with the **7b** were used as control for 24 h and (b, c) treatment with compound **7b** (10 μM) for 12 and 24 h, respectively.

electrophoresis in an agarose gel.[24] This ladder-like pattern is regarded as the biochemical hallmark of apoptosis.[25] Herein, we used agarose gel electrophoresis to detect the DNA fragment. The results were shown in Figure 5. As shown in Figure 5, compared with the control (lane 1), the addition of compounds **7b** (lanes 2, 3 and 4) lead to more obvious ladder-like pattern bands, indicating that compounds **7b** could induce apoptosis against HeLa cell lines. The result was well consistent with that of fluorescence staining and TUNEL assay.

The apoptosis ratios induced by compound **7b** in HeLa tumor cells were then quantitatively determined by flow cytometry (Fig. 6). Four quadrant images were observed by flow cytometric analysis: the Q1 area represented damaged cells appearing in the process of cell collection, the Q2 region showed necrotic cells

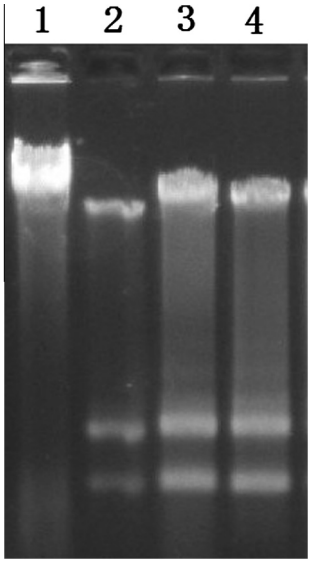

Figure 5. DNA ladder assay. Compound **7b** induced apoptosis-associated DNA fragmentation in HeLa cells. The electrophoretic gel images of total cellular DNA extracted from compound **7b** treated HeLa cells and normal cultural HeLa cells. HeLa cells were treated with compound **7b** at 5, 10 and 15 μM for 24 h, respectively. The lane 1 was a normal cultural HeLa cells as control, and lane 2 was treated with compound **7b** at 5 μM; lane 3 was treated with compound **7b** at 10 μM; lane 4 was treated with compound **7b** at 15 μM, respectively.

and later period apoptotic cells, the Q3 area exhibited normal cells, and the early apoptotic cells were located in the Q4 area. Figure 6 revealed that compound **7b** could induce apoptosis in HeLa cells. Apoptosis ratios (including the early and late apoptosis ratios) for compound **7b** were obtained after 12 h of treatment at the concentration of 5 and 10 μM. The apoptosis of HeLa cells treated with compound **7b** increased gradually in a concentration manner. The apoptosis ratios of compound **7b** measured at different concentration points were found to 12.6%(5 μM) and 33.7%(10 μM), respectively, while that of control was 2.3%. The results obviously illustrated that compound **7b** suppressed cell proliferation by inducing apoptosis.

Mitochondria plays an important role in cell death by changing its outer and inner membrane permeability and thus leading to cytochrome c release and caspases activation.[26,27] Herein, we demonstrated that compound **7b** could disrupt the function of mitochondria at the early stage of apoptosis and subsequently coordinate caspase activation through the release of cytochrome c. Treatment of HeLa cells was performed with different concentrations of compound **7b** for 12 h. As shown in Figure 7, nuclei with karyopyknosis and conglomeration, a characteristic of apoptosis, were observed under fluorescence microscopy in cells cultured with compound **7b**, while the control cells appeared with regular contours. These results showed that compound **7b** was able to induce a loss of mitochondrial transmembrane potential and release of mitochondrial cytochrome c into the cytosol. Therefore, it could be concluded that the apoptosis induced by compound **7b** in HeLa cells may be through the intrinsic pathway.

Recently, oxidative damage to the mitochondrial membrane due to increased generation of reactive oxygen species (ROS) has been demonstrated to play a important role in apoptosis.[28–30] Mitochondria has also been implicated as a source of ROS during apoptosis. Reduced mitochondria membrane potential has recently been shown to lead to increased generation of ROS and apoptosis.[31] We herein studied the loss of mitochondrial transmembrane potential resulting in the generation of ROS by assessing ROS generation caused by target compound **7b** in vitro, using the fluorescent probe 2,7-dichlorofluorescein diacetate (DCF-DA) determined by fluorescence microscopy. Treated with compound **7b**, cells exhibited stronger fluorescence intensity in cytoplasm, while not treated with compound **7b**, cells under the same experimental procedures were used as control and the fluorescence detected in these cells were weak and spread all over the cells. For fluorescence microscopy, Figure 8 revealed that HeLa cells treated with the compound **7b** appeared in stronger green fluorescence (in the web version), indicating that compound **7b** significantly induced apoptosis against HeLa cell line. This phenomenon implied that the increment of ROS might play a role as an early mediator in compound **7b** induced apoptosis. These findings pointed to an effect of compound **7b** on mitochondrial function and accumulation of ROS. These features were cues for the induction of apoptosis.

It is well-known that an increase of intracellular ROS can lead to apoptosis. On the other hand, a decrease of ROS can also ruin the stability of mitochondria, which is followed by a loss of mitochondrial membrane potential, release of cytochrome c into cytosol, and cascade activation of caspases.[27,28,30,32] The occurrence of the apoptotic process should be confirmed by the presence of caspase-3 and -9 (which played a crucial role and was a key element in the execution phase of apoptosis). The enzyme activities of caspase-3 and -9 were determined by spectrophotometry (Fig. 9). After incubation with compound **7b** for 24 h, the activities of caspase-3 and -9 increased compared with the control. As shown in Figure 9, the results clearly showed that an induction of cell apoptosis took place when the cells were treated with compound **7b**, and the stimulation of caspase-3 and -9 activities both increased in a time dependent manner from 3 to 24 h.

In this study, a series of novel DHA-dipeptide derivatives were designed and synthesized, and their cell growth inhibition activities against the NCI-H460, HepG2, SK-OV-3, BEL-7404, HeLa and HCT-116 cell lines were evaluated using MTT assay. The in vitro antitumor activities screening revealed that many compounds exhibited better inhibition activities than the commercial anticancer drug 5-FU. The apoptosis-inducing activity of representative compound **7b** in HeLa cells were investigated by AO/EB staining,

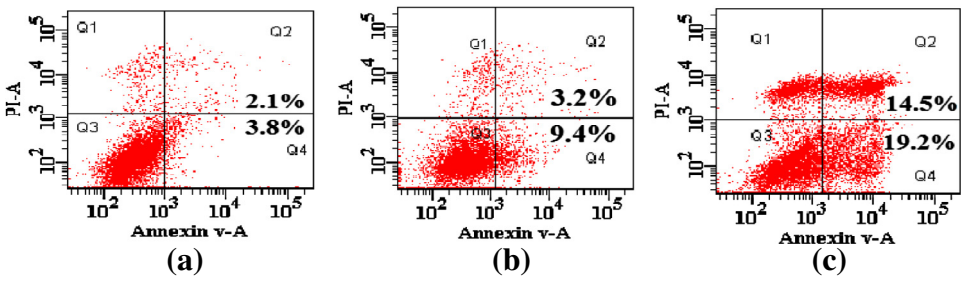

Figure 6. Apoptosis ratio detection of compound **7b** by Annexin V/PI assay. (a) Not treated with the **7b** was used as control for 12 h and (b, c) treatment with compound **7b** at 5 and 10 μM for 12 h, respectively.

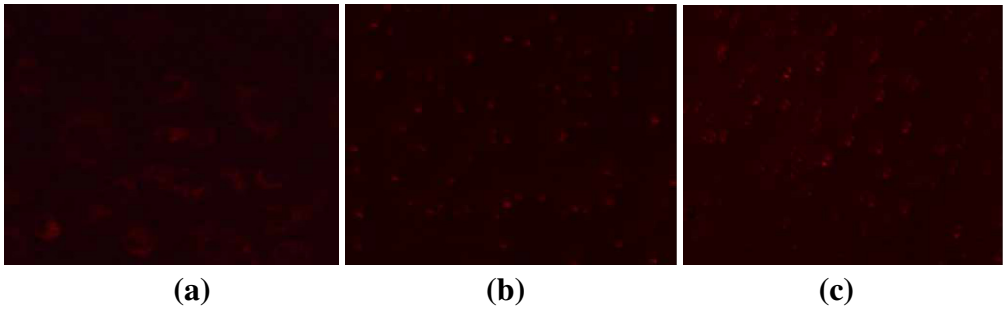

Figure 7. Induction of cytochrome c release assay of compound **7b** in HeLa cells. (a) Not treated with the **7b** were used as control for 12 h and (b, c) treatment with compound **7b** (5, 10 μM) for 12 h, respectively.

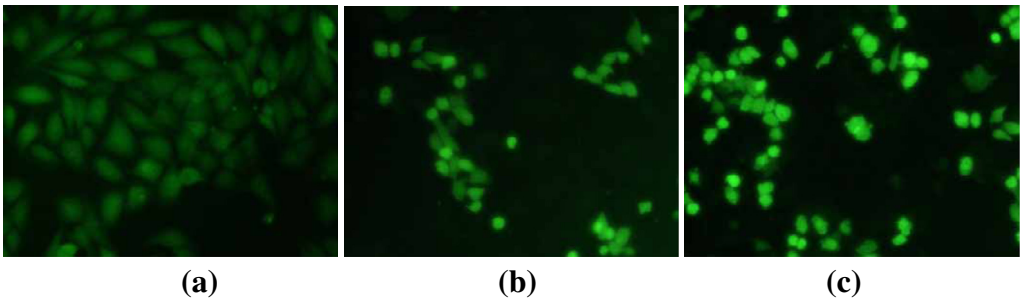

Figure 8. ROS generation assay of compound **7b** in HeLa cells. (a) Not treated with the **7b** were used as control for 12 h and (b, c) treatment with compound **7b** (5, 10 μM) for 12 h, respectively.

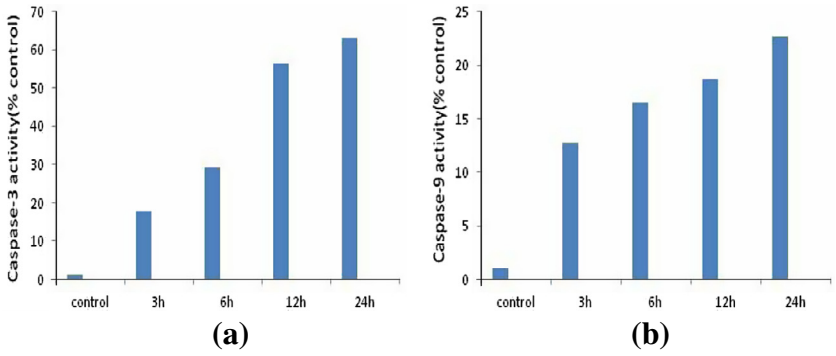

Figure 9. Measurement of caspase-3 and -9 activities. Dose-dependent induction of caspase-3 (a) and -9 (b) in human HeLa cell line.

Hoechst 33258 staining, JC-1 mitochondrial membrane potential staining, TUNEL assay, DNA ladder assay and flow cytometry. Furthermore, compound **7b** was found to induce apoptosis in HeLa cells via the mitochondrial pathway, including a decrease of the reactive oxygen species level, loss of mitochondrial membrane potential, release of cytochrome c, activation of caspase-9 and caspase-3. The above results demonstrate that the rational design of DHA-dipeptide derivatives as novel antitumor leads is feasible. The precise mechanism of action is currently under way.

Acknowledgments

This study was supported by 973 project (No. 2011CB512005, 2012CB723501), the National Natural Science Foundation of China (No. 81260472 and 21362002), Guangxi Natural Science Foundation of China (2011GXNSFD018010 and No. 2010GXNSFF013001), the Guilin Scientific Research and Technological Development Project (No. 20110106-2; 20120108-6), Bagui Scholar project and the Foundation of Ministry of Education Innovation Team (No. IRT1225).

Supplementary data

Supplementary data associated with this article can be found, in the online version, at http://dx.doi.org/10.1016/j.bmcl.2014.02.001.

References and notes

1. Jordan, M. A.; Wilson, L. *Nat. Rev. Cancer* **2004**, *4*, 253.
2. Vennila, R.; Kamalraj, S.; Muthumary, J. *Biomed. Aging Pathol.* **2012**, *2*, 16.
3. Noble, R. L.; Beer, C. T.; Cutts, J. H. *Ann. N.Y. Acad. Sci.* **1958**, *76*, 882.
4. Moncrief, J. W.; Lipscomb, W. N. *J. Am. Chem. Soc.* **1965**, *87*, 4963.
5. Neuss, N.; Neuss, M. N. In *The Alkaloids*; Brossi, A., Suffness, M., Eds.; Academic: San Diego, 1990; Vol. 37, p 229.
6. Newman, D. J.; Cragg, G. M.; Snader, K. M. *J. Nat. Prod.* **2003**, *66*, 1022.
7. (a) Lin, C. -H.; Chuang, H. -S. U.S. Patent 5, 248, 696, 2003.; (b) Zhou, B.; Miao, Z.-H.; Deng, G.; Ding, J.; Yang, Y.-X.; Feng, H.-J.; Li, Y.-Y. *Bioorg. Med. Chem. Lett.* **2010**, *20*, 6217–6221.
8. (a) Huang, X.-C.; Wang, M.; Pan, Y.-M.; Tian, X.-Y.; Wang, H.-S.; Zhang, Y. *Bioorg. Med. Chem. Lett.* **2013**, *23*, 5283; (b) Huang, X.-C.; Wang, M.; Pan, Y.-M.; Yao, G.-Y.; Wang, H.-S.; Tian, X.-Y.; Qin, J.-K.; Zhang, Y. *Eur. J. Med. Chem.* **2013**, *69*, 508.

9. (a) Nielsen, P. E. *Pseudo-peptides in Drug Discovery*; Wiley: New York, 2004; (b) Leader, B.; Baca, Q. J.; Golan, D. E. *Nat. Rev. Drug Disc.* **2008**, *7*, 21; (c) Hancock, R. E. W.; Scott, M. G. *Proc. Natl. Acad. Sci. U.S.A.* **2000**, *97*, 8856.
10. Masquelier, M.; Baurain, R.; Trouet, A. *J. Med. Chem.* **1980**, *23*, 1166.
11. Ryppa, C.; Steinberg, H.; Biniossek, M.; Fainaro, R.; Kratz, F. *Int. J. Pharm.* **2009**, *368*, 89.
12. Zitzmann, S.; Ehemann, V.; Schwab, M. *Cancer Res.* **2002**, *62*, 5139.
13. Al-Hazimi, H. M.; El-Faham, A.; Ghazzali, M.; Al-Farhan, K. *Arab. J. Chem.* **2012**, *5*, 285.

14. (a) *General procedure for the preparation of compounds* **7***:* Compound **2** (1 mmol) added to dry CH_2Cl_2 (15 mL) was stirred at 0 °C and oxalyl chloride (1.5 mmol) was dripped into the mixture and stirred at room temperature for 6 h. After the reaction, the solvent and excess oxalyl chloride was evaporated under reduced pressure. Aromatic primary amines (1 mmol) and triethylamine (0.5 mmol) were added to the mixture and stirred at room temperature for 0.5 h. After the reaction, the solvent was evaporated under reduced pressure, and the crude product was purified by chromatography on silica gel eluted with petroleum ether/ethyl acetate (*V*:*V* = 6:1) to offer compound **4**. Compound **4** (1 mmol) and hydrazine hydrate (3 mmol) were added to ethanol (15 mL) and the mixture was stirred at room temperature for 8 h. After the reaction was completed, the solvent was evaporated under reduced pressure, and the crude product was purified by chromatography on silica gel eluted with petroleum ether/ethyl acetate (*V*:*V* = 3:1) to obtain compounds **5**. DHA (1 mmol) added to dry CH_2Cl_2 (15 mL) was stirred at 0 °C and oxalyl chloride (1.5 mmol) was dripped into the mixture and stirred at room temperature for 6 h. After the reaction, the solvent and excess oxalyl chloride was evaporated under reduced pressure. Compounds **5** (1 mmol) and triethylamine (0.5 mmol) were added to the mixture and stirred at room temperature for 0.5 h. After the reaction, the solvent was evaporated under reduced pressure, and the crude product was purified by chromatography on silica gel eluted with petroleum ether/ethyl acetate (*V*:*V* = 6:1) to offer compounds **7a**–**7s**; (b) *Experimental:* NMR spectra were recorded on a BRUKER AVANCE 500 NMR spectrometer in $CDCl_3$. Mass spectra were determined on a FTMS ESI spectrometer. Compound **7a**: Yields 92%, ^{1}H NMR (400 MHz, $CDCl_3$): δ 8.97 (s, 1H, NH), 7.40 (d, *J* = 7.5 Hz, 2H), 7.24 (d, *J* = 2.5 Hz, 3H), 7.21 (d, *J* = 8.2 Hz, 2H), 7.16 (d, *J* = 8.2 Hz, 1H), 7.07 (d, *J* = 7.4 Hz, 1H), 7.04–6.97 (m, 2H), 6.84 (d, *J* = 1.4 Hz, 1H), 6.69 (d, *J* = 7.7 Hz, 1H), 5.06 (dd, *J* = 14.2, 8.1 Hz, 1H), 3.29–3.12 (m, 2H), 2.86–2.71 (m, 3H), 2.29 (d, *J* = 12.6 Hz, 1H), 2.13 (d, *J* = 12.5, 1H), 1.74–1.45 (m, 7H), 1.25 (s, 3H, CH_3), 1.23 (d, *J* = 2.8 Hz, 6H, 2 × CH_3), 1.19 (s, 3H, CH_3). ^{13}C NMR (100 MHz, $CDCl_3$): δ 179.47, 169.87, 146.82, 145.68, 137.64, 136.83, 134.53, 129.33, 128.80, 128.66, 127.01, 126.89, 124.26, 124.00, 123.87, 120.12, 55.43, 47.40, 45.19, 38.17, 37.88, 37.03, 36.95, 33.48, 29.92, 25.17, 24.02, 20.82, 18.60, 16.39. HRMS (*m*/*z*) (ESI): calcd for $C_{35}H_{42}N_2O_2$ [M+Na$^+$]: 545.31440; found: 545.31005; Compound **7b**: Yields 85.56%; ^{1}H NMR (400 MHz, $CDCl_3$): δ 8.74 (s, 1H), 7.29 (d, *J* = 2.2 Hz, 1H), 7.27 (d, *J* = 2.3 Hz, 2H), 7.26 (d, *J* = 3.6 Hz, 3H), 7.15 (d, *J* = 8.2 Hz, 1H), 7.00 (dd, *J* = 8.1, 1.7 Hz, 1H), 6.84 (d, *J* = 1.5 Hz, 1H), 6.75 (d, *J* = 9.0 Hz, 2H), 6.66 (d, *J* = 7.5 Hz, 1H), 5.01 (dd, *J* = 14.3, 7.8 Hz, 1H), 3.77 (s, 3H, Ph-OCH_3), 3.26–3.12 (m, 2H), 2.86–2.71 (m, 3H), 2.27 (d, *J* = 12.4 Hz, 1H), 2.15–2.08 (m, 1H), 1.75–1.44 (m, 7H), 1.24 (d, *J* = 1.9 Hz, 6H, 2 × CH_3), 1.22 (s, 3H, CH_3), 1.19 (s, 3H, CH_3). ^{13}C NMR (100 MHz, $CDCl_3$): δ 179.30, 169.49, 156.36, 146.84, 145.68, 136.83, 134.56, 130.71, 129.36, 128.66, 126.99, 126.88, 124.01, 123.87, 121.87, 113.96, 55.43, 55.27, 47.36, 45.20, 38.28, 37.86, 37.02, 36.99, 33.46, 29.96, 25.17, 24.00, 20.83, 18.59, 16.37. HRMS (*m*/*z*) (ESI): calcd for $C_{36}H_{44}N_2O_3$ [M+Na$^+$]: 575.32496; found: 575.32104; Compound **7c**: Yields 83.28%; ^{1}H NMR (400 MHz, $CDCl_3$): δ 9.07 (s, 1H, NH), 7.44–7.41 (m, 2H), 7.36–7.32 (m, 3H), 7.24 (d, *J* = 8.2 Hz, 1H), 7.10 (dd, *J* = 8.2, 1.7 Hz, 2H), 6.98 (d, *J* = 8.8 Hz, 2H), 6.93 (d, *J* = 1.5 Hz, 1H), 6.77 (d, *J* = 7.6 Hz, 1H), 5.10 (dd, *J* = 14.5, 8.0 Hz, 1H), 3.34–3.20 (m, 2H), 2.97–2.80 (m, 3H), 2.40 (d, *J* = 1.9 Hz, 1H), 2.20–2.15 (m, 1H), 1.76–1.61 (dd, *J* = 32.7, 20.6 Hz, 7H), 1.33 (d, *J* = 2.1 Hz, 6H, 2 × CH_3), 1.32 (s, 3H, CH_3), 1.28 (s, 3H, CH_3). ^{13}C NMR (100 MHz, $CDCl_3$): δ 179.65, 169.77, 146.76, 145.76, 136.64, 134.47, 133.62, 129.26, 128.73, 127.08, 126.86, 124.15, 124.02, 123.93, 121.81, 121.73, 115.53, 115.31, 55.38, 47.41, 45.20, 37.91, 36.98, 33.46, 29.91, 25.15, 23.99, 20.79, 18.58, 16.33. HRMS (*m*/*z*) (ESI): calcd for $C_{35}H_{41}FN_2O_2$ [M+Na$^+$]: 563.30498; found: 563.30241; Compound **7d**: Yields 85.42%; ^{1}H NMR (400 MHz, $CDCl_3$): δ 9.09 (s, 1H, NH), 7.34–7.31 (m, 2H), 7.23(dd, *J* = 7.6 Hz, 2H), 7.16 (dd, *J* = 7.3 Hz, 2H), 7.14 (dd, *J* = 5.6 Hz, 2H), 7.04–6.93 (m, 2H), 6.85 (d, *J* = 1.3 Hz, 1H), 6.62 (d, *J* = 7.6 Hz, 1H), 5.03 (dd, *J* = 14.1, 8.1 Hz, 1H), 3.27–3.09 (m, 2H), 2.86–2.70 (m, 3H), 2.29 (d, *J* = 12.4 Hz, 1H), 2.10 (dd, *J* = 12.5, 1.8 Hz, 1H), 1.73–1.48 (m, 7H), 1.25 (d, *J* = 2.1 Hz, 6H, 2 × CH_3), 1.23 (s, 3H, CH_3), 1.19 (s, 3H, CH_3). ^{13}C NMR (100 MHz, $CDCl_3$): δ 179.58, 169.70, 146.71, 145.81, 136.54, 136.24, 134.36, 129.24, 128.76, 128.68, 128.39, 127.08, 126.87, 123.98, 121.21, 121.06, 55.39, 47.45, 45.22, 38.24, 37.85, 37.61, 37.10, 36.92, 33.45, 29.88, 25.13, 23.98, 20.81, 18.55, 16.34. HRMS (*m*/*z*) (ESI): calcd for $C_{35}H_{41}ClN_2O_2$ [M+Na$^+$]: 579.27543; found: 579.27190; Compound **7e**: Yields 87.58%; ^{1}H NMR (400 MHz, $CDCl_3$): δ 8.49 (s, 1H, NH), 8.33 (d, *J* = 8.3 Hz, 1H), 7.35–7.33 (m, 1H), 7.33–2.27(m, 3H), 7.25 (t, *J* = 4.1 Hz, 2H), 7.15 (dd, *J* = 8.2, 4.6 Hz, 1H), 7.05 (dd, *J* = 7.7, 4.1, Hz, 1H), 7.02–6.96 (m, 1H), 6.84 (s, 1H), 6.37 (d, *J* = 12.5 Hz, 1H), 4.95 (t, *J* = 7.3 Hz, 1H), 3.34–3.12 (m, 2H), 2.88–2.65 (m, 3H), 2.28 (dd, *J* = 8.2, 4.9 Hz, 1H), 2.12–2.04 (m, 1H), 1.76–1.39 (m, 7H), 1.25 (s, 3H, CH_3), 1.22 (d, *J* = 2.6 Hz, 6H, 2 × CH_3), 1.20 (s, 3H, CH_3). ^{13}C NMR (100 MHz, $CDCl_3$): δ 179.25, 169.66, 146.77, 145.71, 136.54, 136.32, 134.57, 134.37, 129.21, 129.15, 128.91, 128.84, 127.53, 127.19, 126.88, 126.82, 124.91, 123.94, 123.83, 121.81, 55.38, 47.43, 45.34, 45.16, 37.82, 37.53, 36.95, 33.45, 29.68, 25.15, 23.97, 21.23, 20.70, 18.59, 16.32. HRMS (*m*/*z*) (ESI): calcd for $C_{35}H_{41}ClN_2O_2$ [M+Na$^+$]: 579.27543; found: 579.27102; Compound **7f**: Yields 84.21%; ^{1}H NMR (400 MHz, $CDCl_3$): δ 9.20 (s, 1H, NH), 7.31 (s, 1H), 7.27 (d, *J* = 2.9 Hz, 2H), 7.24 (d, *J* = 2.1 Hz, 1H), 7.17 (d, *J* = 11.8 Hz, 2H), 7.14 (s, 1H), 7.04–7.00 (m, 3H), 6.91 (s, 1H), 6.83 (dd, *J* = 14.3, 3.7 Hz, 2H), 5.31 (s, 1H, NH), 5.04 (dd, *J* = 14.4, 8.4 Hz, 1H), 3.24–3.06 (m, 2H), 2.88–2.76 (m, 3H), 2.30 (d, *J* = 1.9 Hz, 1H), 2.10 (d, *J* = 3.9 Hz, 1H), 1.67–1.50 (m, 7H), 1.31 (s, 3H, CH_3), 1.25 (d, *J* = 4.6 Hz, 6H, 2 × CH_3), 1.23 (s, 3H, CH_3). ^{13}C NMR (100 MHz, $CDCl_3$): δ 179.87, 170.04, 146.74, 145.70, 136.72, 136.52, 134.71, 134.41, 131.74, 129.23, 128.71, 127.13, 126.92, 124.15, 124.04, 123.96, 123.91, 121.59, 55.46, 47.45, 47.35, 45.25, 44.68 , 37.87, 36.96, 33.48, 30.04, 25.15, 24.01, 20.68, 18.58, 16.32. HRMS (*m*/*z*) (ESI): calcd for $C_{35}H_{41}BrN_2O_2$ [M+Na$^+$]: 623.22491; found: 623.22068; Compound **7g**: Yields 86.42%; ^{1}H NMR (400 MHz, $CDCl_3$): δ 9.17 (s, 1H, NH), 7.33 (d, *J* = 2.1 Hz, 1H), 7.31 (d, *J* = 2.0 Hz, 1H), 7.25 (d, *J* = 2.3 Hz, 2H), 7.23 (d, *J* = 2.6 Hz, 2H), 7.15 (d, *J* = 3.4 Hz, 2H), 7.08–6.99 (m, 2H), 6.85 (d, *J* = 1.4 Hz, 1H), 6.65 (d, *J* = 7.3 Hz, 1H), 5.04 (dd, *J* = 10.4, 7.4 Hz, 1H), 3.26–3.07 (m, 2H), 2.87–2.69 (m, 3H), 2.29 (d, *J* = 12.4 Hz, 1H), 2.11 (d, *J* = 11.7 Hz, 1H), 1.76–1.49 (m, 7H), 1.25 (*J* = 2.1 Hz, 6H, 2 × CH_3), 1.23 (s, 3H,), 1.19 (s, 3H, CH_3). ^{13}C NMR (100 MHz, $CDCl_3$): δ 179.61, 169.78, 146.74, 145.81, 136.55, 136.26, 134.38, 129.25, 129.18, 128.76, 128.68, 127.09, 126.88, 123.99, 121.23, 121.09, 55.40, 47.45, 45.21, 38.30, 37.86, 37.02, 33.46, 29.89, 25.14, 24.11, 24.01, 23.94, 20.82, 18.56, 16.35. HRMS (*m*/*z*) (ESI): calcd for $C_{36}H_{41}F_3N_2O_2$ [M+Na$^+$]: 613.30178; found: 613.29834; Compound **7h**: Yields 85.23%; ^{1}H NMR (400 MHz, $CDCl_3$): δ 8.89 (s, 1H, NH), 7.27 (d, *J* = 3.9 Hz, 2H), 7.16 (s, 1H), 7.14 (d, *J* = 3.7 Hz, 1H), 7.11 (d, *J* = 8.1 Hz, 1H), 7.00 (dd, *J* = 8.1, 1.7 Hz, 1H), 6.91–6.76 (m, 3H), 6.69 (d, *J* = 7.7 Hz, 1H), 6.63 (dd, *J* = 8.2, 1.9 Hz, 1H), 5.01 (dd, *J* = 14.4, 8.1 Hz, 1H), 3.76 (s, 3H, Ph-OCH_3), 3.27–3.09 (m, 2H), 2.85–2.69 (m, 3H), 2.28 (d, *J* = 12.7 Hz, 1H), 2.09 (d, *J* = 12.5 Hz, 1H), 1.72–1.48 (m, 7H), 1.24 (s, 3H, CH_3), 1.23 (d, *J* = 2.8 Hz, 6H, 2 × CH_3), 1.18 (s, 3H, CH_3). ^{13}C NMR (100 MHz, $CDCl_3$): δ 179.55, 169.87, 159.97, 146.88, 145.68, 138.82, 136.76, 134.54, 129.50, 129.28, 128.72, 127.03, 126.87, 124.06, 123.88, 112.30, 110.42, 105.54 , 55.51, 55.23, 47.41, 45.30, 37.89 (d, *J* = 9.5 Hz), 36.89, 33.47, 29.93, 25.18, 24.00, 20.76, 18.60, 16.34. HRMS (*m*/*z*) (ESI): calcd for $C_{36}H_{44}N_2O_3$ [M+Na$^+$]: 575.32496; found: 575.32074; Compound **7i**: Yields 86.62%; ^{1}H NMR (400 MHz, $CDCl_3$): δ 8.87 (s, 1H, NH), 7.27 (dd, *J* = 7.8, 2.6 Hz, 2H), 7.23 (d, *J* = 3.5 Hz, 2H), 7.21 (s, 1H), 7.15 (d, *J* = 8.2 Hz, 1H), 7.11 (dd, *J* = 7.2, 4.4 Hz, 2H), 7.00 (dd, *J* = 8.1, 1.8 Hz, 1H), 6.89 (d, *J* = 7.5 Hz, 1H), 6.84 (d, *J* = 1.5 Hz, 1H), 6.67 (d, *J* = 7.7 Hz, 1H), 5.05 (dd, *J* = 14.2, 8.1 Hz, 1H), 3.27–3.12 (m, 2H), 2.85–2.71 (m, 3H), 2.28 (s, 3H, Ph-CH_3), 2.20 (d, *J* = 12.5 Hz, 1H), 2.12 (dd, *J* = 12.5, 1.8 Hz, 1H), 1.78–1.51 (m, 7H), 1.25 (s, 3H, CH_3), 1.24 (d, *J* = 7.0 Hz, 6H, 2 × CH_3), 1.20 (s, 3H, CH_3). ^{13}C NMR (100 MHz, $CDCl_3$): δ 179.45, 169.71, 146.81, 145.69, 138.66, 137.56, 136.81, 134.50, 129.34, 128.67, 128.63, 127.00, 126.86, 125.09, 124.02, 123.89, 120.75, 117.21, 55.41, 47.41, 45.31, 38.33, 37.89, 36.98, 33.45, 29.96, 25.20, 24.01, 21.39, 20.83, 18.62, 16.37. HRMS (*m*/*z*) (ESI): calcd for $C_{36}H_{44}N_2O_2$ [M+Na$^+$]: 559.33005; found: 559.32629; Compound **7j**: Yields 86.37%; ^{1}H NMR (400 MHz, $CDCl_3$): δ 9.20 (s, 1H, NH), 7.37 (d, *J* = 10.9 Hz, 1H), 7.23 (d, *J* = 5.4 Hz, 2H), 7.14 (t, *J* = 3.1 Hz, 2H), 7.10 (t, *J* = 5.7 Hz, 1H), 7.03–6.99 (m, 2H), 6.83 (t, *J* = 5.0 Hz, 1H), 6.80–6.72 (m, 2H), 6.67 (d, *J* = 7.8 Hz, 1H), 5.06 (dd, *J* = 7.9, 2.6 Hz, 1H), 3.2–3.04 (m, 2H), 2.84–2.69 (m, 3H), 2.30 (d, *J* = 12.6 Hz, 1H), 2.10 (dd, *J* = 12.5, 1.8 Hz, 1H), 1.77–1.54 (m, 7H), 1.26 (s, 3H, CH_3), 1.24 (d, *J* = 6.9 Hz, 6H, 2 × CH_3), 1.20 (s, 3H, CH_3). ^{13}C NMR (100 MHz, $CDCl_3$): δ 179.61, 169.87, 146.73, 145.74, 139.22, 136.57, 134.42, 129.86, 129.75, 129.22, 128.66, 128.44, 127.07, 126.89, 123.99, 123.92, 115.29, 110.98, 55.43, 47.55, 47.48, 45.27, 38.29, 37.86, 37.08, 36.95, 33.45 , 29.86, 25.20, 23.98, 20.79, 18.57, 16.35. HRMS (*m*/*z*) (ESI): calcd for $C_{35}H_{41}FN_2O_2$ [M+Na$^+$]: 563.30498; found: 563.30137; Compound **7k**: Yields 85.54%; ^{1}H NMR (400 MHz, $CDCl_3$): δ 9.24 (s, 1H, NH), 7.47 (d, *J* = 1.9 Hz, 1H), 7.22 (dd, *J* = 7.4, 2.3 Hz, 2H), 7.16 (d, *J* = 4.6 Hz, 2H), 7.11–7.07 (m, 1H), 7.03–7.00 (m, 2H), 6.87 (dd, *J* = 20.5, 5.8 Hz, 2H), 6.80–6.67 (m, 2H), 5.08 (dd, *J* = 8.0, 3.1 Hz, 1H), 3.23–3.01 (m, 2H), 2.82 (dd, *J* = 14.2, 7.3 Hz, 3H), 2.32 (d, *J* = 7.3 Hz, 1H), 2.09 (dd, *J* = 12.5, 1.8 Hz, 1H), 1.77–1.59 (m, 7H), 1.27 (s, 3H, CH_3), 1.25 (d, *J* = 2.1 Hz, 6H, 2 × CH_3), 1.22 (s, 3H, CH_3). ^{13}C NMR (100 MHz, $CDCl_3$): δ 179.54, 169.87, 146.72, 145.76, 145.74, 138.88, 136.58, 134.41, 134.34, 129.74, 129.22, 128.63, 128.44, 127.07, 126.90, 124.02, 120.11, 117.91, 55.43, 47.45, 46.88, 45.33, 38.55, 38.21, 36.97, 33.48, 29.84, 25.23, 24.01, 21.26, 20.82, 18.58, 16.38. HRMS (*m*/*z*) (ESI): calcd for $C_{35}H_{41}ClN_2O_2$ [M+Na$^+$]: 579.27543; found: 579.27095; Compound **7l**: Yields 84.55%; ^{1}H NMR (400 MHz, $CDCl_3$): δ 9.25 (s, 1H, NH), 7.73 (d, *J* = 1.9 Hz, 1H), 7.33 (d, *J* = 3.3 Hz, 2H), 7.28 (d, *J* = 3.1 Hz, 2H), 7.18 (d, *J* = 8.0 Hz, 1H), 7.11–7.09 (m, 2H), 6.99 (d, *J* = 7.1 Hz, 2H), 6.94 (d, *J* = 1.5 Hz, 1H), 6.83 (d, *J* = 7.7 Hz, 1H), 5.12 (dd, *J* = 15.3, 7.6 Hz, 1H), 3.44–3.21 (m, 2H), 2.81 (d, *J* = 6.3 Hz, 3H), 2.40 (d, *J* = 1.6 Hz, 1H), 2.15 (d, *J* = 1.8 Hz, 1H), 1.73–1.62 (m, 7H), 1.39 (s, 3H, CH_3), 1.34 (s, 6H, 2 × CH_3), 1.32 (s, 3H, CH_3). ^{13}C NMR (100 MHz, $CDCl_3$): δ 179.74, 170.04, 146.84, 145.73, 139.01, 136.59, 134.69, 134.47, 130.06, 129.22, 128.69, 127.21, 127.01, 126.69, 124.11, 124.02, 122.95, 122.39, 118.44, 55.50, 49.02, 47.50, 45.23, 44.72, 37.81 , 37.00, 36.89, 33.45, 29.91, 25.11, 23.98, 21.78, 18.60, 16.33. HRMS (*m*/*z*) (ESI): calcd for $C_{35}H_{41}BrN_2O_2$ [M+Na$^+$]: 623.22491; found: 623.22116; Compound **7m**: Yields 89.37%; ^{1}H NMR (400 MHz, $CDCl_3$): δ 9.87 (s, 1H, NH), 8.23 (t, *J* = 2.1 Hz, 1H), 7.44 (d, *J* = 8.2 Hz, 1H), 7.29 (d, *J* = 2.0 Hz, 3H), 7.20 (d, *J* = 2.9 Hz, 2H), 7.13–7.08 (m, 2H), 7.01 (t, *J* = 5.4 Hz, 1H), 6.94 (d, *J* = 1.3 Hz, 1H), 6.86 (dd, *J* = 11.5, 4.6 Hz, 1H), 5.40 (s, 1H, NH), 5.28 (dd, *J* = 7.9, 4.5 Hz, 1H), 3.38–3.25 (m, 2H), 2.94–2.81 (m, 3H), 2.41 (d, *J* = 2.6, 1H), 2.27 (d, *J* = 2.3 Hz, 1H), 1.87–1.72 (m, 7H), 1.40 (s, 3H), 1.34 (d, *J* = 2.3 Hz, 6H, 2 × CH_3), 1.31 (s, 3H, CH_3). ^{13}C NMR (100 MHz, $CDCl_3$): δ 179.89, 170.29, 148.33, 146.69, 145.85, 139.00, 136.41, 134.28, 129.48, 129.15, 128.64, 128.50, 127.12, 126.88, 125.41, 124.02, 118.61, 114.70, 55.50, 47.68, 47.60, 45.47, 37.31, 37.00, 33.39, 29.86, 25.28, 25.15, 24.00, 20.87, 18.58, 16.37. HRMS (*m*/*z*) (ESI): calcd for $C_{35}H_{41}N_3O_4$ [M+Na$^+$]: 590.29948; found: 590.29563; Compound **7n**: Yields 85.49%; ^{1}H NMR (400 MHz, $CDCl_3$): δ 8.83 (s, 1H, NH), 7.37–7.35 (m, 4H), 7.25

(d, J = 8.6 Hz, 3H), 7.08 (d, J = 9.2 Hz, 2H), 6.94 (d, J = 1.2 Hz, 1H), 6.77 (d, J = 7.7 Hz, 1H), 5.40 (s, 1H, NH), 5.12 (dd, J = 14.3, 8.0 Hz, 1H), 3.36−3.26 (m, 2H), 2.95–2.80 (m, 3H), 2.40 (d, J = 2.8 Hz, 1H), 2.30 (s, 3H, CH_3-Ph), 2.27 (s, 3H, CH_3-Ph), 2.20 (d, J = 3.2 Hz, 1H), 1.89–1.58 (m, 7H), 1.34 (d, J = 2.1 Hz, 6H, 2 × CH_3), 1.32 (s, 3H, CH_3), 1.29 (s, 3H, CH_3). ^{13}C NMR (100 MHz, $CDCl_3$): δ 179.28, 169.55, 146.83, 145.67, 136.98, 136.88, 135.33, 134.58, 132.57, 129.78, 129.37, 128.65, 126.97, 126.88, 124.03, 123.86, 121.47, 117.67, 55.36, 53.46, 47.39, 45.27, 38.29, 37.88, 36.99, 33.47, 29.99, 25.21, 24.01, 20.84, 19.77, 19.18, 18.62, 16.40. HRMS (m/z) (ESI): calcd for $C_{37}H_{46}N_2O_2$ [M+Na$^+$]: 573.34570; found: 573.34132; Compound **7o**: Yields 85.52%; ^{1}H NMR (400 MHz, $CDCl_3$): δ 9.20 (s, 1H, NH), 7.69 (d, J = 2.1 Hz, 1H), 7.29 (d, J = 5.6 Hz, 2H), 7.24 (d, J = 6.7 Hz, 2H), 7.15 (d, J = 10.6 Hz, 1H), 7.13–7.07 (m, 2H), 7.00–6.95 (m, 1H), 6.90 (s, 1H), 6.80 (d, J = 7.8 Hz, 1H), 5.14 (dd, J = 14.1, 8.1 Hz, 1H), 3.29–3.08 (m, 2H), 2.96–2.74 (m, 4H), 2.38 (s, 3H, Ph-CH_3), 2.23(d, J = 10.8 Hz, 1H), 1.81–1.52 (m, 7H), 1.37 (s, 3H, CH_3), 1.32 (d, J = 4.4 Hz, 6H, 2 × CH_3), 1.30 (s, 3H, CH_3). ^{13}C NMR (100 MHz, $CDCl_3$): δ 179.45, 169.59, 146.75, 145.65, 136.52 , 134.37, 131.64, 130.67, 129.26, 129.17, 128.61, 128.55, 127.04, 126.89, 123.92, 120.69, 120.44, 118.14, 55.33, 54.96, 47.47, 38.39, 37.86, 36.99, 29.77, 25.17, 23.95, 21.19, 19.41, 18.59, 16.36. HRMS (m/z) (ESI): calcd for $C_{36}H_{43}ClN_2O_2$ [M+Na$^+$]: 593.29108; found: 593.28748; Compound **7p**: Yields 86.76%; ^{1}H NMR (400 MHz, $CDCl_3$): δ 9.47 (s, 1H, NH), 7.67 (d, J = 2.1 Hz, 1H), 7.34 (d, J = 7.8 Hz, 2H), 7.29 (d, J = 5.6 Hz, 2H), 7.24 (s, 1H), 7.12–7.08 (m, 2H), 7.01–6.93 (m, 2H), 6.72 (d, J = 7.6 Hz, 1H), 5.11 (dd, J = 6.7, 2.3 Hz, 1H), 3.36–3.12 (m, 2H), 2.97–2.80 (m, 3H), 2.81 (d, J = 6.6 Hz, 1H), 2.40 (d, J = 10.8 Hz, 1H), 1.82–1.65 (m, 7H), 1.35 (s, 3H, CH_3), 1.33 (d, J = 4.2 Hz, 6H, 2 × CH_3), 1.29 (s, 3H, CH_3). ^{13}C NMR (100 MHz, $CDCl_3$): δ 180.07, 169.91, 146.56, 145.72, 137.26, 136.42, 134.35, 132.49, 130.22, 129.13, 128.74, 127.28, 127.15, 127.03, 126.87, 123.99, 121.51, 119.01, 60.20, 55.55, 47.42, 45.39, 42.16, 37.98, 37.87, 37.12, 36.98, 33.44, 29.88, 25.13, 23.96, 20.82, 18.48, 16.34. HRMS (m/z) (ESI): calcd for $C_{35}H_{40}Cl_2N_2O_2$ [M+Na$^+$]: 613.23645; found: 613.23269; Compound **7q**: Yields 85.58%; ^{1}H NMR (400 MHz, $CDCl_3$): δ 9.33 (s, 1H, NH), 7.51 (dd, J = 6.6, 2.6 Hz, 1H), 7.25 (d, J = 7.3 Hz, 2H), 7.21–7.19 (m, 2H), 7.14 (s, 1H), 7.03–6.98 (m, 2H), 6.94 (d, J = 8.8 Hz, 1H), 6.85 (d, J = 1.4 Hz, 1H), 6.67 (d, J = 7.7 Hz, 1H), 5.05 (dd, J = 8.9, 5.7 Hz, 1H), 3.24–3.02 (m, 2H), 2.87–2.67 (m, 3H), 2.31 (d, J = 11.4 Hz, 1H), 2.09 (dd, J = 12.7, 2.0 Hz, 1H), 1.73–1.52 (m, 7H), 1.27 (s, 3H, CH_3), 1.24 (d, J = 4.9 Hz, 6H, 2 × CH_3), 1.20 (s, 3H, CH_3). ^{13}C NMR (100 MHz, $CDCl_3$): δ 179.78, 169.88, 146.67, 145.85, 136.49, 134.45, 134.35, 129.18, 128.67, 128.42, 127.10, 126.89, 124.01, 122.09, 119.53, 119.47, 116.38, 116.11, 55.46, 54.73, 47.50, 45.36, 42.24, 38.57 37.90, 37.17, 36.69, 33.46, 29.88, 25.14, 23.95, 20.85, 18.57, 16.38. HRMS (m/z) (ESI): calcd for $C_{35}H_{40}FCl_2N_2O_2$ [M+Na$^+$]: 597.26600; found: 597.262089; Compound **7r**: Yields 86.36%; ^{1}H NMR (400 MHz, $CDCl_3$): δ 8.24 (s, 1H, NH), 8.08 (d, J = 3.0 Hz, 1H), 7.31 (s, 1H), 7.27 (d, J = 2.6 Hz, 2H), 7.15 (d, J = 8.2 Hz, 2H), 6.76 (dd, J = 8.9, 3.0 Hz, 2H), 6.59 (dd, J = 8.9, 3.5 Hz, 2H), 6.42 (d, J = 7.4 Hz, 1H), 4.90 (d, J = 7.2 Hz, 1H), 3.80 (s, 3H, Ph-OCH_3), 3.71 (s, 3H, Ph-OCH_3), 3.22–3.17 (m, 2H), 2.84–2.73 (m, 3H), 2.29 (d, J = 12.4 Hz, 1H), 2.12–2.09 (m, 1H), 1.77–1.56 (m, 7H), 1.24 (s, 3H, CH_3), 1.23 (d, J = 1.9 Hz, 6H, 2 × CH_3), 1.20 (s, 3H, CH_3). ^{13}C NMR (100 MHz, $CDCl_3$): δ 178.68, 169.22, 153.73, 146.81, 145.66, 142.31, 136.69, 134.66, 129.28, 128.77, 127.80, 127.02, 123.99, 123.82, 110.83, 108.82, 106.03, 56.17, 55.78, 55.39, 47.37, 45.15, 38.02, 37.87, 36.98, 33.46, 29.92, 25.16, 23.99, 20.75, 18.66, 16.36. HRMS (m/z) (ESI): calcd for $C_{37}H_{46}N_2O_4$ [M+Na$^+$]: 605.33553; found: 605.33052; Compound **7s**: Yields 85.37%; ^{1}H NMR (400 MHz, $CDCl_3$): δ 8.59 (s, 1H, NH), 8.46 (d, J = 1.9 Hz, 1H), 7.33 (d, J = 0.6 Hz, 1H), 7.28 (d, J = 1.9 Hz, 2H), 7.27 (d, J = 2.3 Hz, 2H), 7.14 (d, J = 3.2 Hz, 1H), 7.05–7.03 (m, 1H), 6.99 (d, J = 6.1 Hz, 1H), 6.84 (d, J = 1.3 Hz, 2H), 6.34 (d, J = 7.3 Hz, 1H), 4.90 (dd, J = 7.0, 2.2 Hz, 1H), 3.14 (dd, J = 14.2, 8.3 Hz, 2H), 2.85–2.67 (m, 3H), 2.29 (d, J = 5.4 Hz, 1H), 2.08 (d, J = 2.2 Hz, 1H), 1.54–1.31 (m, 7H), 1.24 (s, 3H, CH_3), 1.20 (d, J = 3.0 Hz, 6H, 2 × CH_3), 1.17 (s, 3H, CH_3). ^{13}C NMR (100 MHz, $CDCl_3$): δ 179.41, 169.85, 146.70, 145.73, 136.36, 136.14, 135.28, 134.49, 133.30, 129.78, 129.17, 129.10, 128.91, 127.27, 126.88, 124.73, 123.96, 121.41, 55.39, 47.43, 45.17, 37.80, 37.18, 36.97, 33.46, 29.65, 25.17, 23.99, 21.25, 20.63, 18.60, 16.36. HRMS (m/z) (ESI): calcd for $C_{35}H_{40}Cl_2N_2O_2$ [M+Na$^+$]: 613.23645; found: 613.23241.

15. *General procedure for cytotoxic evaluation in vitro:* NCI-H460, HepG2, SK-OV-3, BEL-7404, HeLa and HCT-116 cells were seeded into 96-well microculture plates and allowed to adhere for 24 h, respectively. After cells were exposed to compounds at concentrations from 100 to 0.01 μM for 48 h, medium was aspirated and replenished with complete medium. IC_{50} was evaluated by MTT tetrazolium dye assay. Each experiment was performed three times; (c) Statistical analysis: All statistical analysis was performed with SPSS Version 10. Data was analyzed by one-way ANOVA. Mean separations were performed using the least significant difference method. Each experiment was replicated thrice, and all experiments yielded similar results. Measurements from all the replicates were combined, and treatment effects were analyzed.
16. Bunz, F. *Curr. Opin. Pharmacol.* **2001**, *1*, 337.
17. *General procedure for AO/EB staining:* cells were seeded at a concentration of 5 × 10^4 cell/ mL in a volume of 2 mL on a sterile cover slip in six-well tissue culture plates. Following incubation, the medium was removed and replaced with fresh medium plus 10% fetal bovine serum and supplemented with compound **7c** (5 μM). After the treatment period, the cover slip with monolayer cells was inverted on a glass slide with 20 μL of AO/EB stain (100 mg/mL). Fluorescence was read on an Nikon ECLIPSETE2000-S fluorescence microscope (OLYMPUS Co., Japan).
18. *General procedure for Hoechst 33258 staining:* cells grown on a sterile cover slip in six-well tissue culture plates were treated with compounds for a certain range of time. The culture medium containing compounds was removed, and the cells were fixed in 4% paraformaldehyde for 10 min. After being washed twice with PBS, the cells were stained with 0.5 mL of Hoechst 33258 (Beyotime) for 5 min and then again washed twice with PBS. The stained nuclei were observed under an Nikon ECLIPSETE2000-S fluorescence microscope using 350 nm excitation and 460 nm emission.
19. *General procedure for mitochondrial membrane potential staining:* JC-1 probe was employed to measure mitochondrial depolarization in NCI-H460 cells. Briefly, cells cultured in six-well plates after indicated treatments were incubated with an equal volume of JC-1 staining solution (5 μg/ml) at 37 °C for 20 min and rinsed twice with PBS. Mitochondrial membrane potentials were monitored by determining the relative amounts of dual emissions from mitochondrial JC-1 monomers or aggregates using an Nikon ECLIPSETE2000-S fluorescent microscope. Mitochondrial depolarization is indicated by an increase in the green/red fluorescence intensity ratio.
20. The TUNEL method was performed to label 3′-end of fragmented DNA of the apoptotic HeLa cells. The cells treated as indicated were fixed with 4% paraform phosphate buffer saline, rinsed with PBS, then permeabilized by 0.1% Triton X-100 for FITC end-labeling the fragmented DNA of the apoptotic HeLa cells using TUNEL cell apoptosis detection kit. The FITC-labeled TUNEL-positive cells were imaged under a fluorescent microscopy by using 488 nm excitation and 530 nm emission.
21. (a) *General procedure apoptosis ratios:* Prepared NCI-H460 cells (1 × 10^6 cells/ mL) were washed twice with cold PBS and then resuspended gently in 500 μL of binding buffer. Thereafter, cells were stained in 5 μL of Annexin V-FITC and shaken well. Finally, the cells were mixed with 5 μL of PI, incubated for 20 min in the dark and subsequently analyzed using FACSCali-bur (Becton Dickinson).; (b) *General procedure cell cycle:* NCI-H460 cell lines were maintained in Dulbecco's modified Eagle's medium with 10% foetal calf serum in 5% CO_2 at 37 °C. Cells were harvested by trypsinization and rinsed with PBS. After centrifugation, the pellet (10^5–10^6 cells) was suspended in 1 mL of PBS and kept on ice for 5 min. The cell suspensionwas then fixed by the dropwise addition of 9 mL precooled (4 °C) 75% ethanol with violent shaking. Fixed samples were kept at 4 °C until use. For staining, cells were centrifuged, resuspended in PBS, digested with 500 μL of RNase A (250 mg/mL), and treated with 25 μL of propidium iodide (PI) (0.15 mM), then incubated for 30 min at 4 °C. PI-positive cells were counted with a FACScan Fluorescence-activated cell sorter (FACS). The population of cells in each cell-cycle phase was determined using Cell Modi FIT software (Becton Dickinson).; (c) Tong, G.; Poot, M.; Hu, D.; Oda, D. *Oral Oncol.* **2000**, *36*, 236.
22. Halicka, H. D.; Bedner, E.; Darzynkiewicz, Z. *Exp. Cell Res.* **2000**, *260*, 248.
23. Yasuhara, S.; Zhu, Y.; Matsui, T.; Tipirneni, N.; Yasuhara, Y. K.; Kaneki, M.; Rosenzweig, A.; Martyn, J. A. J.; Histochem, J. *Cytochemistry* **2003**, *51*, 873.
24. Wyllie, A. H. *Nature* **1980**, *284*, 555.
25. Samali, A.; Gorman, A. M.; Cotter, T. G. *Experientia* **1996**, *52*, 933.
26. Bose, J. S.; Gangan, V.; Prakash, R.; Jain, S. K.; Manna, S. K. *J. Med. Chem.* **2009**, *52*, 3184.
27. Fang, Z. X.; Liao, P. C.; Yang, Y. L.; Yang, F. L.; Chen, Y. L.; Lam, Y. L.; Hua, K. F.; Wu, S.-H. *J. Med. Chem.* **2010**, *53*, 7967.
28. Zhang, J. Y.; Wu, H. Y.; Xia, X. K.; Liang, Y. J.; Yan, Y. Y.; She, Z. G.; Lin, Y. C.; Fu, L. W. *Cancer Biol. Ther.* **2007**, *6*, 1413.
29. Quan, Z.; Gu, J.; Dong, P.; Lu, J.; Wu, X.; Wu, W.; Fei, X.; Li, S.; Wang, Y.; Wang, J.; Liu, Y. *Cancer Lett.* **2010**, *295*, 252.
30. Wang, X. H.; Jia, D. Z.; Liang, Y. J.; Yan, S. L.; Ding, Y.; Chen, L. M.; Shi, Z.; Zeng, M. S.; Liu, G. F.; Fu, L. W. *Cancer Lett.* **2007**, *249*, 256.
31. Zamzami, N.; Marchetti, P.; Castedo, M.; Decaudin, D.; Macho, A.; Hirsch, T.; Susin, S. A.; Petit, P. X.; Mignotte, B.; Kroemer, G. *J. Exp. Med.* **1995**, *182*, 367.
32. Zhang, J. Y.; Yi, T.; Liu, J.; Zhao, Z. Z.; Chen, H. B. *J. Agric. Food Chem.* **2013**, *61*, 2188.